



Strongly confining bare core CdTe quantum dots in polymeric microdisk resonators

Assegid Flatae, Tobias Grossmann, Torsten Beck, Sarah Wiegele, and Heinz Kalt

Citation: *APL Materials* **2**, 012107 (2014); doi: 10.1063/1.4862695

View online: <http://dx.doi.org/10.1063/1.4862695>

View Table of Contents: <http://scitation.aip.org/content/aip/journal/aplmater/2/1?ver=pdfcov>

Published by the [AIP Publishing](#)

Articles you may be interested in

[Surface plasmon enhanced Förster resonance energy transfer between the CdTe quantum dots](#)

Appl. Phys. Lett. **93**, 123102 (2008); 10.1063/1.2981209

[Investigation of the Quantum Confinement Effects in CdTe Dots by Electrical Measurements](#)

AIP Conf. Proc. **893**, 813 (2007); 10.1063/1.2730139

[CdSe quantum dot microdisk laser](#)

Appl. Phys. Lett. **89**, 231104 (2006); 10.1063/1.2402263

[Whispering gallery modes in high quality Zn Se Zn Mg S Se microdisks with CdSe quantum dots studied at room temperature](#)

Appl. Phys. Lett. **89**, 091105 (2006); 10.1063/1.2345236

[Optical loss and lasing characteristics of high-quality-factor AlGaAs microdisk resonators with embedded quantum dots](#)

Appl. Phys. Lett. **86**, 151106 (2005); 10.1063/1.1901810

AIP | Journal of Applied Physics



Journal of Applied Physics is pleased to announce **André Anders** as its new Editor-in-Chief

Strongly confining bare core CdTe quantum dots in polymeric microdisk resonators

Assegid Flatae,^a Tobias Grossmann, Torsten Beck, Sarah Wiegele, and Heinz Kalt

Institute of Applied Physics and DFG-Center for Functional Nanostructures (CFN), Karlsruhe Institute of Technology (KIT), Wolfgang-Gaede-Str.1, 76131 Karlsruhe, Germany

(Received 20 October 2013; accepted 3 January 2014; published online 21 January 2014)

We report on a simple route to the efficient coupling of optical emission from strongly confining bare core CdTe quantum dots (QDs) to the eigenmodes of a micro-resonator. The quantum emitters are embedded into QD/polymer sandwich microdisk cavities. This prevents photo-oxidation and yields the high dot concentration necessary to overcome Auger enhanced surface trapping of carriers. In combination with the very high cavity Q-factors, interaction of the QDs with the cavity modes in the weak coupling regime is readily observed. Under nanosecond pulsed excitation the CdTe QDs in the microdisks show lasing with a threshold energy as low as $0.33 \mu\text{J}$. © 2014 Author(s). All article content, except where otherwise noted, is licensed under a Creative Commons Attribution 3.0 Unported License. [<http://dx.doi.org/10.1063/1.4862695>]

In the past few years high quality factor (Q-factor) and small mode volume cavities attracted lots of attention for their potential applications as laser sources,^{1,2} filters,³ and label free bio-sensors⁴ as well as for the study of weak and strong coupling between the quantum emitters and cavity photons (e.g., Purcell effect, cavity quantum electrodynamics effects).^{5,6} For these studies researchers use various types of microresonators like distributed feedback resonators,⁷ plasmonic cavities,⁸ Fabry-Perot cavities,⁹ or whispering gallery mode (WGM) resonators.¹⁰ WGM resonators are well suited for emitter-photon coupling experiments because of their intrinsically high Q-factor. There are various ways to position quantum emitters into or to the rim of WGM resonators.^{2,6,11–15} The most straightforward way to achieve efficient emitter-photon coupling is to place the emitter right into the field maxima of the resonator mode. This is most easily achieved in polymeric WGM resonators where the emitters like laser dyes can be incorporated into the polymer solution before fabrication of the resonators.¹

Colloidal QDs can be very efficient quantum emitters. QD lasing was achieved in the early 1990s^{16,17} and there has been significant improvement in lowering the threshold intensity and increasing the temperature stability of the lasing. Competition between radiative and nonradiative relaxation mechanisms has a big effect on the optical gain required for lasing. This is typically related to the size and the surface properties of the QDs. In small nanocrystalline QDs (in the strongly confined regime where the QDs size is smaller than the Bohr excitonic radius) nonradiative carrier losses are dominated by surface trapping and multiparticle Auger recombination.¹⁸ Upon reducing the size of the QDs the confinement effect increases resulting in a larger splitting of band-edge states¹⁹ and in an enhancement of nonradiative Auger processes.²⁰ For obtaining optical gain and achieve lasing, the concentration of the QDs is an important factor. The Auger loss which is basically related to the biexcitonic population inversion can be overcome by using a high concentration of QDs thus making the stimulated emission build up faster than the Auger decay, the latter having typical time scales of few picoseconds.²⁰ Furthermore, due to the nanoscale size, the QDs have a large surface to volume ratio which has a huge impact on their optical properties. The surface has vacant states which can react with the environment. Photo-oxidation is a typical mechanism quenching the

^aElectronic mail: assegid.flatae@kit.edu



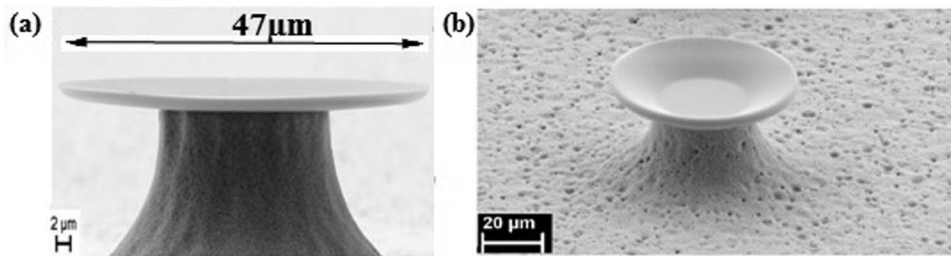


FIG. 1. (a) High-Q PMMA microdisk WGM resonator. After exposure and development of the PMMA, the Si substrate is etched isotropically by XeF_2 leaving PMMA disks standing on silicon pedestals. (b) Heating the microdisks above the glass transition temperature of PMMA (heat reflow process) leads to the formation of microgoblets, which have smoother surfaces and the Q-factor is one order of magnitude higher than for the microdisks. Reprinted with permission from Appl. Phys. Lett. **96**, 013303 (2010). Copyright 2010 AIP Publishing LLC.

photon emission.²¹ Therefore, surface passivation is indispensable to obtain high quantum yield. Quantum dots with a coated core (core/shell type of QDs) have a reduced surface trapping and produce room temperature photoluminescence (PL) with high quantum efficiency within the entire visible wavelength range.^{22,23}

Following the above discussion it is obvious that research on the coupling of strongly confining bare core QDs (e.g., bare core CdTe QDs) to the eigenmodes of the WGM cavities is challenging. Such bare core QDs show a quick bleaching of the emission due to photo-oxidation (as in water droplet WGM resonators¹¹) or due to carrier trapping by surface enhanced Auger effect (Auger decay).²⁰ As a result the QDs do not show lasing for both continuous wave (cw) and pulsed pumping as the damage threshold of this type of QDs is much lower than the one for lasing.^{11,15,24}

The attempt to dope polymer matrix with the QDs is difficult due to the phase separation of the emitters from the polymer matrix. So it is necessary to add special ligands to the QDs surface in order to maximize the solubility of colloidal QDs. In this paper we present a route to achieve efficient coupling of bare core CdTe QDs emission (in the strongly confined regime) with the eigenmodes of microdisk cavities. By the use of QD/polymer sandwich WGM resonators we are able to incorporate a high density of emitters, shield them from photo-oxidation and place them in the maximum of the resonator modes. The integration mechanism does not require surface functionalization of the emitters and enables the CdTe QDs to be easily coupled to the optical mode of the cavity. The coupling is evidenced by the observation of periodic narrow peaks of WGMs on the bulk emission of the QDs and by low-threshold lasing.

The CdTe QDs we used in our experiments (Plasma Chem, Berlin) easily form a colloidal solution in water and are terminated with a $-\text{COOH}$ group. The nanoparticles have a size of 3.3 nm which is smaller than the excitonic Bohr radius of CdTe (~ 7.3 nm).²⁵ Hence, the emitters are in the strongly confining regime and their electronic states are separated much more than the available thermal energy inhibiting thermal de-population of the lowest electronic states. The emission peak wavelength of the QDs is in between 580 and 590 nm.

The achievement of lasing requires the CdTe QDs to be integrated into a high-quality feedback cavity. We fabricated microdisk and microgoblet resonators made of the polymer poly(methyl methacrylate) (PMMA) on a silicon (Si) substrate. The PMMA (MicroChem PMMA 950k A7, dissolved in anisole) is spin coated on a silicon wafer (with a PMMA layer thickness of nearly 1 μm). The sample is heated to 110 °C to reduce the solvent content. Then we spin coat three layers of 9 μM water soluble CdTe QDs. Heating the sample at 110 °C for 15–20 s reduces the water content. Once again spin coating PMMA (in anisole) on the QD layers results in a high concentration of CdTe QDs sandwiched between two PMMA layers. We now write the circular resonator patterns on the PMMA-QDs-PMMA layer using e-beam lithography (with a dose current of 1 nA). After this exposure and development of the PMMA, we isotropically etch the exposed Si with XeF_2 . This results in PMMA microdisks standing on Si pedestals, as shown in Figure 1(a). The resonators used in this work have a diameter of 26 μm and 47 μm in size. More on the fabrication steps and techniques to achieve high Q-factor for passive resonators is discussed in Ref. 10.

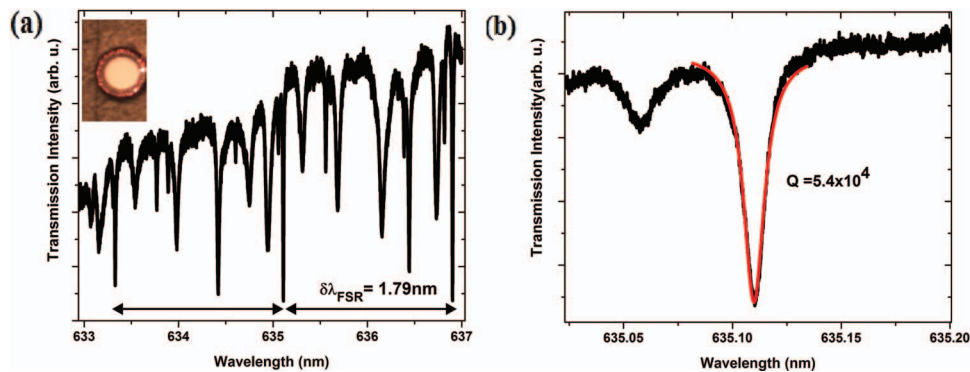


FIG. 2. Mode spectrum and Q-factor of microdisk resonator of diameter $47 \mu\text{m}$ in the 630 nm wavelength range. (a) Transmission spectrum through an evanescently coupled tapered fiber shows WGM resonances. The tapered part of the fiber is brought close to the cavity (inset). The transmitted light from a tunable diode laser which is continuously swept is collected via a photodiode. The measured free spectral range around 635.1 nm is $\delta\lambda_{\text{FSR}} = 1.79 \text{ nm}$. (b) Lorentzian-fit of the mode at about 635.1 nm reveals a Q-factor of 5.4×10^4 .

WGM resonators confine the optical field of the fundamental modes near the rim of the cavities,¹⁰ which results in very high Q-factors. Our sandwiched cavities incorporating QDs have Q-factors of about 5.4×10^4 at wavelength around 635.1 nm. The Q-factor can be increased by one order of magnitude if we apply a thermal reflow step to reduce the surface roughness (surface tension-enhanced thermal reflow) which results in a goblet shaped cavity,¹⁰ as depicted in Figure 1(b). The Q-factor of cavities containing QDs is actually lower than the one for passive disks due to the absorption of cavity photons by the CdTe QDs. The Q-factor is measured from the full width at half maximum of the Lorentzian-shaped resonances observed from the transmission spectra collected from evanescently coupled tapered fiber. The free spectral range (evaluated from the periodic repetition of the modal pattern) near 635.1 nm wavelength range is 1.79 nm, as shown in Figure 2(a). This is in agreement with the theoretically expected value of 1.83 nm for a 47- μm diameter polymeric disk. Besides the fundamental modes, we also observe numerous higher order modes.

The fluorescence measurements were done in a free-space micro-photoluminescence ($\mu\text{-PL}$) setup. The schematic diagram is shown in Figure 3. The pump laser beam is focused on the sample at an angle 45° with respect to normal of the sample's surface. The microcavities were pumped either with cw emission at 432 nm from a HeCd laser or pulses from a frequency-doubled Nd:YVO₄ laser with pulse width of 10-ns and a wavelength of 532 nm. The emission from the sample is collected via a microscope objective of $\text{NA} = 0.4$ ($\times 50$) and the exact position of the sample and the excitation spot (diameter $\sim 60 \mu\text{m}$) is monitored by a camera. The spectral output is analyzed using a spectrometer (spectral resolution of 30 pm) equipped with CCD (charge coupled device) camera. The pump intensity for pulsed excitation is controlled by a Pockels cell along with a polarization filter. The cw excitation intensity is adjusted by neutral density filters.

Excitation of the QDs/PMMA sandwich cavities with a cw HeCd laser shows periodic narrow WGM features on top of the bulk emission of the QDs. Figure 4(a) shows the PL intensity from a 26 μm diameter cavity pumped with 8.5 mW cw power. The QDs are homogeneously distributed within the whole PMMA microcavity, the WGM modes however are well confined to the rim of the resonators. So, only a small percentage of the dots are situated within the modal volume but still show a pronounced effect to the spectrum which is dominated by the spontaneous emission of bulk QDs outside the modes. On the higher energy side of the spectrum the modal structure is less pronounced due to the higher re-absorption of the QDs. Again, the observed modal spectrum is quite complex with a free spectral range of $\delta\lambda_{\text{FSR}} = 2.62 \text{ nm}$ at a wavelength of 589.5 nm as indicated by the arrows in Figure 4(a) (right).

After investigation of the WGM resonances, we increase the pump power to observe a possible cw lasing from the sample. The PL shows a certain increase in the fluorescence and emission linewidth of the QDs until 10 mW. Then a further increase in excitation power leads to

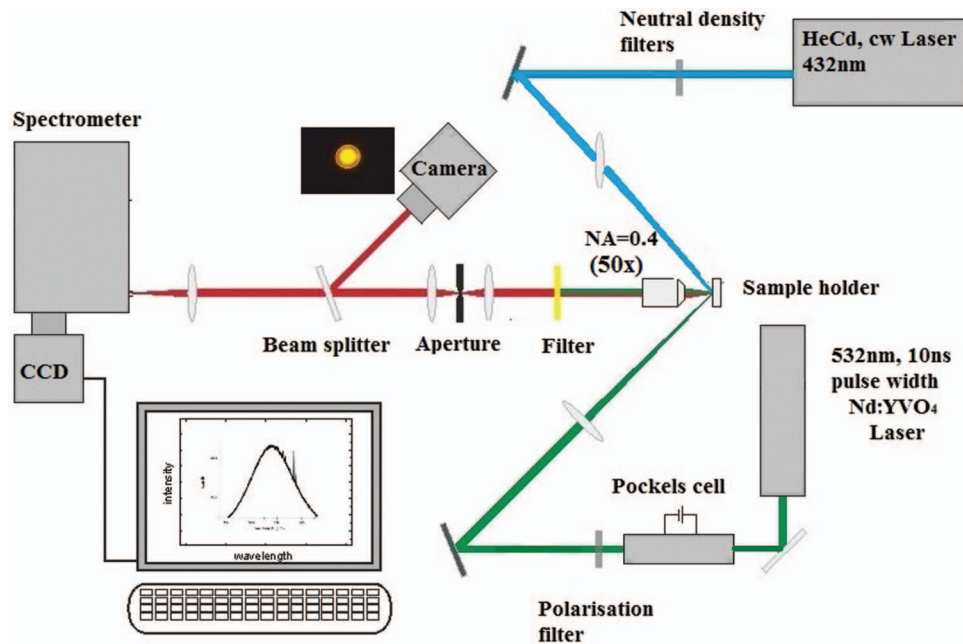


FIG. 3. Micro-photoluminescence setup for free-space excitation measurement using either a cw or a pulsed laser. The pump laser beam is focused onto the sample and the emission from the sample is collected via a microscope objective, monitored on a camera and analyzed by a spectrometer.

photo-bleaching of the QDs. This is manifested by a decrease in PL emission and a blueshift in the peak emission wavelength for an increase in pump energy,^{21,26,27} as depicted in Figure 4(b). The bleaching is irreversible and results in permanent loss of the PL intensity. This kind of irreversible loss of PL intensity of colloidal QDs at high pump powers is typically observed for different kind of QDs.²⁸ It can originate from thermally induced degradation²⁸ and/or charging of the QDs from carrier tunneling or Auger ionization.^{29,30}

The resonant cavity modes also show a blueshift for high excitation power. The shifts observed between two consecutive fundamental modes are not equal hence the free spectral range also changes. Figure 5 shows the shift in the resonance modes and the accompanied change in the free spectral range for two different excitation powers 20 mW and 30 mW (upper and lower PL spectrum, respectively) above the photo-bleaching threshold value. The distance between the two modes observed at 587.34 nm and 590.4 nm is 3.06 nm for a pump power of 20 mW and increasing the excitation power to 30 mW leads blueshift of the modes to 585.85 nm and 588.81 nm, respectively, and a decrease in the spectral distance to 2.96 nm. The resonance wavelength of a given mode depends on the diameter of the cavity, the effective index of refraction, and the surrounding medium. PMMA has a large negative thermo-optic coefficient $dn/dT = -1.05 \times 10^{-4}/K$,³¹ so an increase in temperature of the cavity due to optical pumping is expected to dominate the blueshift of the cavity modes.

Pulsed pump sources can avoid bleaching as compared to cw sources, as the time between pulses enables the relaxation of the excited states of the QDs and also pulsed excitation is helpful to avoid Auger process that compete with stimulated emission.^{2,20} Therefore, the threshold condition for the lasing phenomena can be obtained without charging or even destroying the QDs. This is particularly true for the high concentrations of QDs in the sandwich resonator structures. Here it is also important that the bare core dots show a PL efficiency (under low power ns-excitation) that is more than a factor of two smaller than for the QDs embedded into the sandwich structures.

Microcavities pumped with 10-ns laser pulses at 532 nm (with a repetition rate of 70 Hz) show a well-defined onset of lasing. A power law fit to the integrated lasing modes shows a threshold pump energy of 0.33 μJ for a 47 μm diameter microdisk (Figure 6(b)). This threshold value is comparable to the one reported for CdSe/ZnS (core/shell) QDs in microdrop cavities ($\sim 0.4 \mu\text{J}$).¹¹ It was previously reported that by reducing the concentration of the emitters on the surface of the

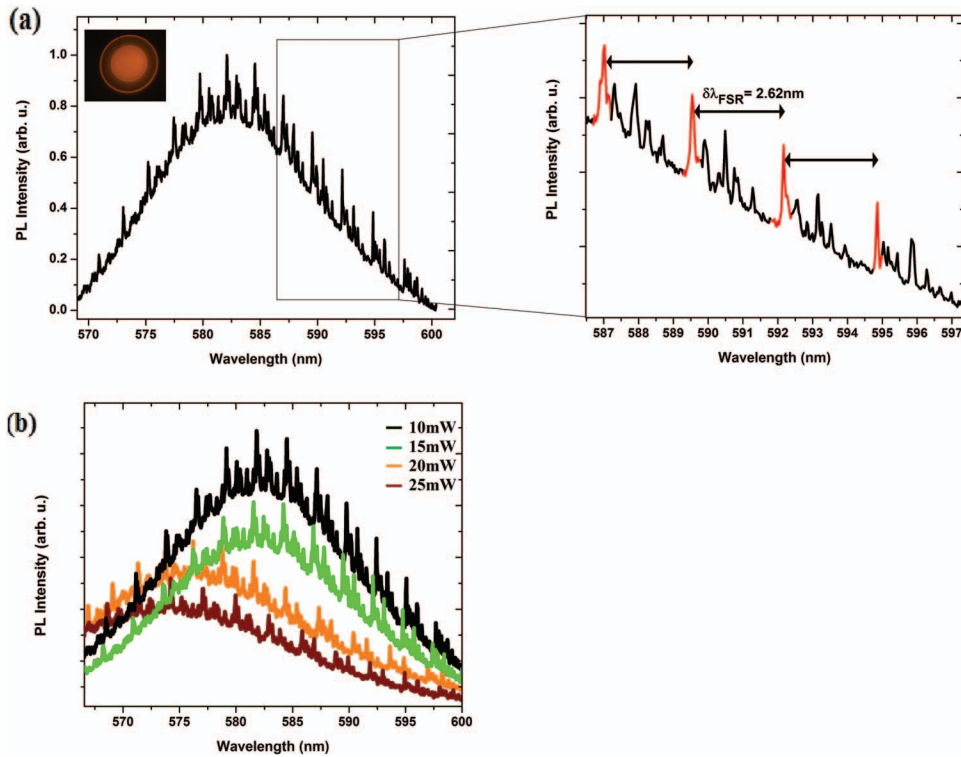


FIG. 4. (a) PL spectrum of CdTe QDs integrated into polymeric sandwich microcavity of diameter $26 \mu\text{m}$. The WGM features are clearly observed on the photoluminescence background of QDs for 8.5 mW cw pump power. The mode structures are complex as shown on the left side of (a), the red peaks show the consecutive azimuthal modes and the arrows show the free spectral range of the resonant mode ($\delta\lambda_{\text{FSR}} = 2.62 \text{ nm}$ near 589.5 nm). The inset on the left of (a) shows the fluorescence image of the QD/PMMA sandwich microdisk. (b) The spontaneous emission increases with cw excitation power up to 10 mW. A further increase in the power leads to a decrease in PL of the QDs bulk emission and a blueshift in the peak emission wavelength of QDs.

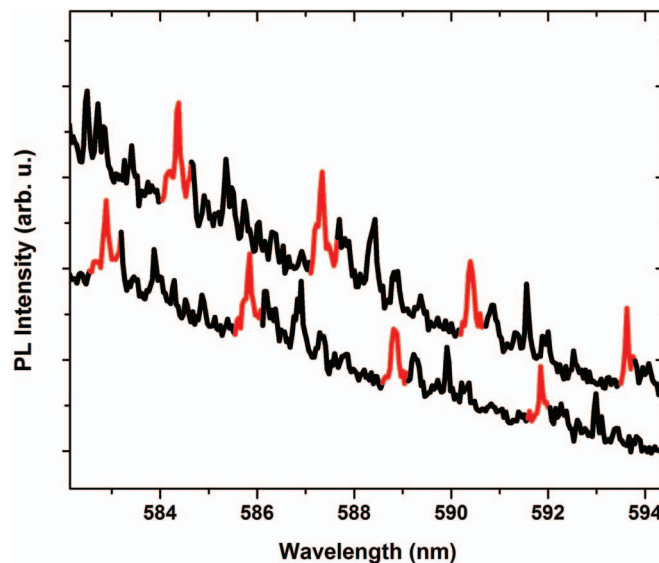


FIG. 5. Blueshifting of the resonance modes for high excitation power. The upper (lower) spectrum is recorded at 20 mW (30 mW) cw excitation power. The red color shows the fundamental WGM modes.

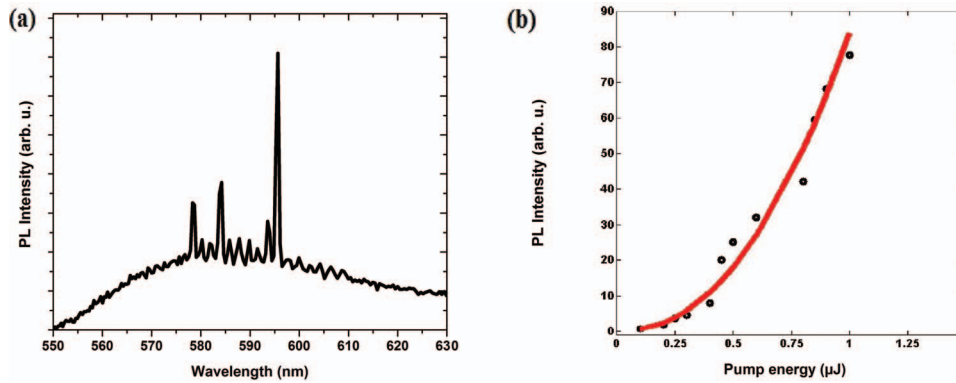


FIG. 6. (a) Lasing spectrum of CdTe QDs/PMMA sandwich microresonator of diameter $47 \mu\text{m}$ at pump energy of $0.5 \mu\text{J}$, above the lasing threshold. (b) A power law fit to the integrated lasing-mode intensity indicates lasing with small threshold energy of about $0.33 \mu\text{J}$.

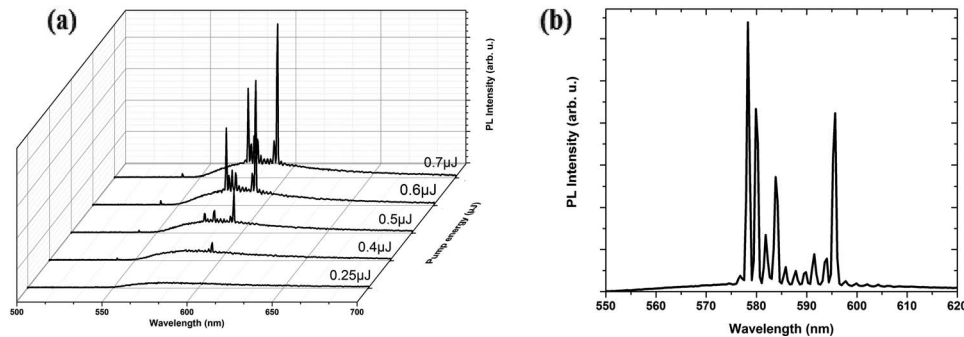


FIG. 7. (a) Room temperature emission-spectra from QDs incorporated into cavities for higher pulsed pump energy is dominated by lasing peaks. The lasing peaks show a stable emission without bleaching and blueshifting. The smaller peak observed near 532 nm is scattered light from the pump pulse. (b) Lasing spectrum recorded at pump energy of $0.9 \mu\text{J}$. A spectral distance of about 2 nm is observed between the lasing modes which correspond to the free spectral range of the cavity modes for a $47 \mu\text{m}$ diameter microdisk.

cavity a reduction in the threshold energy is observed (up to 9.9 fJ for CdSe/ZnS QDs coated on the surface of toroidal microcavity²). As a result of lower quantum yield of the bare core CdTe QDs and enhanced Auger effect associated with its size, a further reduction in the concentration does not yield lasing from CdTe QD/polymer sandwich cavity structures. But a possible reduction in the lasing threshold should be obtainable using tapered fiber excitation due to the efficient pumping of the active gain region of the microdisk cavity as compared to free space excitation. The emission spectrum for higher pump energy is dominated by lasing peaks, as shown in Figure 6(a).

As it is shown in Figure 7(a), the lasing modes are clearly pronounced even for higher pump energy, and also the lasing peaks show no blueshift. The photo-bleaching effects are observed for pump energies higher than $2 \mu\text{J}$, which is far more than the threshold energy necessary for lasing.

Evaluation of the exact spectral positions of the laser peaks is limited by the spectral resolution of the setup. Within these limits we find a fixed mode spacing of about 2 nm for the spectrum at $0.9 \mu\text{J}$ pump energy (Figure 7(b)). This indicates that the lasing most likely occurs in the fundamental cavity modes since they provide highest modal gain as compared to higher order cavity modes. As it is seen from the figure the PL intensity of the lasing modes is different; it must be due to the difference in the number of QD ensembles contributed for the various lasing modes.

In conclusion, we fabricate CdTe QDs/PMMA sandwich microdisk resonators on a silicon chip. The bare core QDs do not need any additional surface functionalization and are well protected in the sandwich structure. Photoluminescence spectra show very narrow, spectrally periodic peaks

evidencing the good coupling to the whispering gallery modes of the microdisks. Under ns pulsed excitation the QDs show lasing with a threshold energy as low as $0.33 \mu\text{J}$.

This work has been supported by the joint Erasmus mundus doctorate program “Europhotonics” frame work agreement (European Contract No. 2010-0001-001/001) and by the Karlsruhe school of optics and photonics (KSOP).

- ¹ T. Grossmann, S. Schleede, M. Hauser, M. B. Christiansen, C. Vannahme, C. Eschenbaum, S. Klinkhammer, T. Beck, J. Fuchs, G. U. Nienhaus, U. Lemmer, A. Kristensen, T. Mappes, and H. Kalt, *Appl. Phys. Lett.* **97**, 063304 (2010).
- ² B. Min, S. Kim, K. Okamoto, L. Yang, A. Scherer, H. Atwater, and K. Vahala, *Appl. Phys. Lett.* **89**, 191124 (2006).
- ³ J. V. Hryniewicz, P. P. Absil, B. E. Little, R. A. Wilson, and P. T. Ho, *IEEE Phot. Tech. Lett.* **12**, 320 (2000).
- ⁴ F. Vollmer and S. Arnold, *Nat. Methods* **5**, 591 (2008).
- ⁵ K. J. Vahala, *Nature (London)* **424**, 839 (2003).
- ⁶ T. J. Kippenberg, A. L. Tchebotareva, J. Kalkman, A. Polman, and K. J. Vahala, *Phys. Rev. Lett.* **103**, 027406 (2009).
- ⁷ I. D. W. Samuel and G. A. Turnbull, *Chem. Rev.* **107**, 1272 (2007).
- ⁸ R. M. Ma, R. F. Oulton, V. J. Sorger, G. Bartal, and X. Zhang, *Nat. Mater.* **10**, 110 (2011).
- ⁹ M. Metcalfe, A. Muller, G. S. Solomon, and J. Lawell, *J. Opt. Soc. Am. B* **26**, 2308 (2009).
- ¹⁰ T. Grossmann, M. Hauser, T. Beck, C. Gohn-Kreuz, M. Karl, H. Kalt, C. Vannahme, and T. Mappes, *Appl. Phys. Lett.* **96**, 013303 (2010).
- ¹¹ J. Schafer, J. P. Mondia, R. Sharma, Z. H. Lu, A. S. Susha, A. L. Rogach, and L. J. Wang, *Nano Lett.* **8**, 1709 (2008).
- ¹² P. T. Snee, Y. Chan, D. G. Nocera, and M. G. Bawendi, *Adv. Mater.* **17**, 1131 (2005).
- ¹³ T. Aoki, B. Dayan, E. Wilcut, W. P. Bowen, A. S. Parkins, T. J. Kippenberg, K. J. Vahala, and H. J. Kimble, *Nature (London)* **443**, 671 (2006).
- ¹⁴ S. I. Shopova, G. Farca, A. T. Rosenberger, W. M. S. Wickramanayake, and N. A. Kotov, *Appl. Phys. Lett.* **85**, 6101 (2004).
- ¹⁵ Y. P. Rakovich, L. Yang, E. M. McCabe, J. F. Donegan, T. Perova, A. Moore, N. Gaponik, and A. Rogach, *Semicond. Sci. Technol.* **18**, 914 (2003).
- ¹⁶ V. V. Vandyshev, V. S. Dneprovskii, V. I. Klimov, and D. K. Okorokov, *JETP Lett.* **54**, 442 (1991).
- ¹⁷ N. N. Ledentsov, V. M. Ustinov, A. Y. Egorov, A. E. Zhukov, M. V. Maksimov, I. G. Tabatadze, and P. S. Kopev, *Semiconductors* **28**, 832 (1994).
- ¹⁸ V. I. Klimov, *J. Phys. Chem. B* **104**, 6112 (2000).
- ¹⁹ V. I. Klimov, A. A. Mikhailovsky, D. W. McBranch, C. A. Leatherdale, and M. G. Bawendi, *Science* **287**, 1011 (2000).
- ²⁰ V. I. Klimov, A. A. Mikhailovsky, S. Xu, A. Malko, J. A. Hollingsworth, C. A. Leatherdale, H. J. Eisler, and M. G. Bawendi, *Science* **290**, 314 (2000).
- ²¹ A. Y. Nazzal, X. Wang, L. Qu, W. Yu, Y. Wang, X. Peng, M. Xiao, *J. Phys. Chem. B* **108**, 5507 (2004).
- ²² M. A. Hines and P. Guyot-Sionnest, *J. Phys. Chem.* **100**, 468 (1996).
- ²³ B. O. Dabbousi, J. R. Viegó, F. V. Mikulec, J. R. Heine, H. Mattoussi, R. Ober, K. F. Jensen, and M. G. Bawendi, *J. Phys. Chem. B* **101**, 9463 (1997).
- ²⁴ R. Sharma, Ph.D. thesis, Max-Planck Institute of Light, Erlangen Nurnberg, 2009.
- ²⁵ V. Esch, B. Fluegel, G. Khitrova, H. M. Gibbs, Xu. Jiajin, K. Kang, S. W. Koch, L. C. Liu, S. H. Risbud, and N. Peyghambarian, *Phys. Rev. B* **42**, 7450 (1990).
- ²⁶ W. G. J. H. M. van Sark, P. L. T. M. Frederix, D. J. Van den Heuvel, H. C. Gerritsen, A. A. Bol, J. N. J. van Lingén, C. D. M. Donega, and A. Meijerink, *J. Phys. Chem. B* **105**, 8281 (2001).
- ²⁷ W. G. J. H. M. van Sark, P. L. T. M. Frederix, A. A. Bol, H. C. Gerritsen, and A. Meijerink, *ChemPhysChem* **3**, 871 (2002).
- ²⁸ Y. Zhao, C. Riemersma, F. Pietra, R. Koole, M. Donega, and A. Meijerink, *ACS Nano* **6**, 9058 (2012).
- ²⁹ M. Kuno, D. P. Fromm, S. T. Johnson, A. Gallagher, and D. J. Nesbitt, *Phys. Rev. B* **67**, 125304 (2003).
- ³⁰ A. L. Efros and M. Rosen, *Phys. Rev. Lett.* **78**, 1110 (1997).
- ³¹ R. M. Waxler, D. Horowitz, and A. Feldman, *Appl. Opt.* **18**, 101 (1979).